Novel Patient-Derived Xenograft and Cell Line Models for Therapeutic Testing of Pediatric Liver Cancer

Beatrice Bissig-Choisat, Claudia Kettlun-Leyton, Xavier D. Legras, Barry Zorman, Mercedes Barzi, Leon L. Chen, Mansi D. Amin, Yung-Hsin Huang, Robia G. Pautler, Oliver A. Hampton, Masand M. Prakash, Diane Yang, Malgorzata Borowiak, Donna Muzny, HarshaVardhan Doddapaneni, Jianhong Hu, Yan Shi, M. Waleed, Gaber, M. John Hicks, Patrick A. Thompson, Yiling Lu, Gordon B. Mills, Milton Finegold, John A. Goss, D. Williams Parsons, Sanjeev A. Vasudevan, Pavel Sumazin, Dolores Lopez-Terrada, Karl-Dimiter Bissig

Table of contents

Supplementary materials and methods

Study design

To establish a patient-derived tumor xenograft (PDTX) model that faithfully recapitulated all aspects of pediatric liver cancer, we sectioned tumors from 15 patients into blocks and engrafted them into 12 to 24 mice per patient tumor sample, depending on the size of the tumor sample and our ability to perform surgical procedures immediately after resection. The size of each tumor sample was restricted by the procedure performed (OLT, hepatectomy, biopsy) and, in some cases, the patient's response to chemotherapy before resection. Sample size, replicates and data collection from specific experiments are described below and in the results section. Data collection was limited by tumor size and occasional morbidity of the animals. No blinded tests were performed.

Animals

Two different mouse strains were used as hosts for PDTX; the NSG (NOD.SCID, Il2rg-/-)[1-4]and the FRG (*fah*$^{-/-}$*, rag2*$^{-/-}$*, Il2rg*$^{-/-}$)[5, 6] strains. Both strains are B, T and NK cell deficient and therefore cannot reject the xenograft.

NSG (NOD.SCID, Il2rg-/-)[1-4] were purchased from Jackson laboratory. The FRG (*fah*$^{-/-}$*, rag2*$^{-/-}$*, Il2rg*$^{-/-}$)[5, 6] strain was kept and utilized as previously described[5, 6]. Both strains were maintained in temperature- and humidity-controlled animal quarters with a 12-hour light/12-hour dark cycle.

MRI Imaging and Analysis

All images in this study were acquired with a 9.4T, Bruker AvanceIII Biospec Spectrometer, 21 cm bore horizontal scanner with a 35mm volume resonator (Bruker Biospin, Billerica, MA). Mice were induced with 5% isoflurane and then maintained on 2% isoflurane in 100% O_2 during imaging. Mice were then placed in a head holder while respiratory rate was monitored and temperature was maintained at 37℃ using an air heating system with the Model 1025 Small Animal Monitoring and Gating System Software (SA Instruments, Inc). For the 2D data sets, the imaging parameters were as follow: an MSME Proton Density spin-spin (T2)-weighted MRI protocol was used. Data sets were collected with a FOV = 4 x 4 cm. Matrix Size = 256 x 256; repetition time (TR) = 8108 ms, Echo Time (TE) = 13 ms. The slice thickness was set at .25 mm with 108 slices; Number of Averages (NA) = 1. For the 3D imaging datasets, the imaging parameters were as follows: TR = 2000ms; TE = 8.365 ms; Rare Factor = 8; FOV = 35 mm x 35 mm x 35 mm. Matrix size = 128 x 128 x 64. NA = 1. Tumors were segmented using the image processing software, AMIRA (Hillsboro, Oregon), and tumor volumes were calculated.

FLT-PET

Forty-five minutes before scanning, each animal was injected intravenously with 1.3 units/g thymidine phosphorylase (TP) flushed with heparin. The TP was injected slowly, over several minutes. The computer tomography (CT) and

positron emission tomography (PET) scans were performed in a docked Siemens Inveon preclinical scanner (Inveon, Siemens AG, Knoxville, TN). Immediately before the PET scan, animals were injected intravenously with 12.58 MBq (340 µCi) of [18F] fluorothymidine (FLT) (Cyclotope, Houston, TX). PET scans were reconstructed using Micro-Q (Siemens AG, Knoxville, TN), using the OSEM-3D algorithm with the attenuation map obtained from the corresponding reconstructed CT scan.

RNA & DNA extraction, RT and PCR

The starting material was 10-20mg of snap frozen tissue tumors were pulverized in liquid nitrogen using a mortar and pestle or 1-3x10^6 cells from cell lines. RNA was extracted using RNAeasy kit (Qiagen) according to manufacturer's protocol. Samples were DNase treated. RNA was stored at -80℃ in aliquots. Total RNA was used for RNA seq and reverse transcription using qScript cDNA SuperMix (Quanta Bioscience), according to manufacturer's protocol. DNA was extracted according to the manufacturer's protocol using the DNAeasy kit (Qiagen). The *NRAS* c181A (Q61K) mutation was amplified by PCR using primers (forward, ACAAACTGGTGGTGGTTGGA and reverse GCACCATAGGTACATCATCCGA primer) flanking the mutation and verified by Sanger sequencing.

Whole exome sequencing (WES)

For the paired-end pre-capture library procedure, both blood and tumor DNA were fragmented by sonicating genomic DNA and ligating to the Illumina multiplexing PE adapters. Whole exome sequencing was performed in the CAP and CLIA-certified Whole Genome Laboratories at BCM following a previously-described protocol[7, 8] including library construction, exome capture by VCRome version 2.1[9] and paired-end sequencing on an Illumina HiSeq instrument. Tumor and germline library pairs were sequenced on a single lane of a HiSeq 2000/2500, with a mean coverage of >250x and a target base coverage of 20x at >97%. Tumor exomes were analyzed using the Mercury v.3 pipeline[10], including variant calling and annotation. A somatic variant list was generated for each patient by subtracting the germline .vcf from the tumor .vcf and applying somatic filters (total coverage in tumor >7, variant coverage in normal <4, variant ratio in normal <5% of variant ratio in tumor, sum of variant base qualities in normal <=70) to the merged file with a tumor variant ratio cut-off >= 0.05. Somatic mutations were annotated with information from the Catalog of Somatic Mutations in Cancer (COSMIC) database (http://cancer.sanger.ac.uk/cosmic)[11]. Somatic variants were imported into an in-house developed variant review program and subjected to additional filters (selection of coding variants predicted to alter protein, intronic variants at +/- 2 bp, and synonymous coding variants predicted to affect splicing) followed by inspection of read alignments on the Integrative Genomics Viewer[12].

RNA-Seq libraries

Whole-transcriptome RNA sequencing (RNA-Seq) was performed using total RNA extracted from fresh-frozen tissue to prepare strand-specific, poly-A+ RNA-Seq libraries for sequencing on the Illumina platform. Briefly, poly-A^+ mRNA was extracted from 1 µg total RNA using Oligo$(dT)_{25}$ Dynabeads (Life Technologies, Cat. No. 61002), followed by fragmentation of the mRNA by heat at 94^{o}C for 3 minutes (for samples with RIN=3 & 3.3) or 4 minutes (for samples with RIN of 6.0 & 6.7). First strand cDNA was synthesized using the Superscript III reverse transcriptase (Life Technologies, Cat. No. 18080-044) and purified using Agencourt RNAClean XP beads (Beckman Coulter, Cat. No. A63987). During second strand cDNA synthesis, dNTP mix containing dUTP was used to introduce strand-specificity. For Illumina paired-end library construction, the resultant cDNA was processed through end-repair and A-tailing, ligated with Illumina PE adapters, and then digested with 10 units of Uracil-DNA Glycosylase (NEB, Cat. No. M0280L). Amplification of the libraries was performed for 13 PCR cycles using the Phusion High-Fidelity PCR Master Mix (NEB, Cat. No. M0531L); 6-bp molecular barcodes were also incorporated during this PCR amplification. The cDNA was purified with Agencourt AMPure XP beads after each enzymatic reaction. After quantification using the Agilent Bioanalyzer 2100 DNA Chip 7500 (Agilent Technilogies, Cat. No. 5067-1506), libraries were pooled in equimolar amounts (2 libraries/pool. The library pools were then loaded onto a HiSeq flowcell lane, and following amplification with Illumina's cBot cluster generation system, sequencing runs were performed in paired-end mode (2 x

100-bp reads) using the Illumina HiSeq 2500 platform. On average, 83.7 million paired reads (166-190 million total reads) were generated per sample.

cDNA libraries from different passages of PDTX#2 were generated and sequenced with an alternative method; total RNA was processed according to the manufacturer's recommendation using the TrueSeq Stranded mRNA LT kit (Illumina) to generate libraries. The libraries were sequenced on a NextSeq 500 sequencer. The average read per sample was 14 millions.

RNA-seq FastQ files were processed using STAR, and Cufflinks and alignment to the Hg19/GRCh37

Unsupervised PCA analysis of RNA expression.

In order to adjust for batch effects between the two types of profiling technologies used, (Illumina genome analyzer and NextSeq sequencers), the xenograft sample (X#1) was profiled by both genome analyzer and NextSeq. The replicates were equated using a multiplicative scaling vector, which was then used to scale all samples of X#1at passages 2, 3, 13 and 20. For PCA analysis, FPKM values for 2438 genes were included after filtering for HGNC protein coding genes with average expression above 25 FPKM and coefficient of variation (CV) above 0.3 over the set of all samples (including cell lines, tumors and xenografts). PCA was implemented in R using the prcomp function with the scale parameter set to adjust variables to unit variance.

Western blotting and ELISA

Cells were plated in a six-well plate and incubated with different concentrations of the MEK-1/2 inhibitor trametinib (GSK1120212) (0.001-1nM) or the pan-PI3K inhibitor buparlisib (NVP-BKM120) (0.0005-100nM). After incubation, cells were lysed using RIPA buffer supplemented with protease inhibitor cocktail (complete Mini, EDTA-free, ROCHE) and passed through a 22G needle. Samples were run in 4-12% Bis-Tris gels (Novex, Life Technology) with MOPS buffer. Transfer to PVDF membrane and probed for total ERK (137F5, Cell Signaling) and P-ERK (D13.14.4E, Cell Signaling), total AKT (C67E7, Cell Signaling), P-AKT (D9E, Cell Signaling) and β-Actin (AC-15, Sigma Aldrich).

ELISA for human albumin (Bethyl laboratories) and human AFP (DRG-Diagnostics) were performed using dilutions of 1:10-10,000 (depending on time after transplantation) according to manufacturer's recommendations.

Immunostaining and detection of EdU

Immunostaining was done from paraffin embedded (β-catenin, glypican-3) or cryopreserved (vWF, MECA32, human nuclear staining) tissue blocks. Tissue was fixed by 4% PFA either over night before embedding (paraffin) or for 10 min (cryopreservation) immediately before immunostaining. Paraffin sections were dewaxed and antigen retrieval (15 min in citrate buffer pH6.0) was performed for MECA32 and human nuclear antibody co-staining only. Co-staining was performed in PBS, 0.5% BSA, 0.02% TritonX100 using antibodies against vWF (dilution 1:400, Abcam) or MECA32 (dilution 1:50, Novus Biologicals, #NB100-

77668), and human nuclei (dilution 1:250, Millipore). After washing in PBS, the sections were stained with fluorescent-labeled secondary antibodies (Jackson Immunoresearch Laboratories) and mounted with Vectashield plus DAPI (Vector Labs). Staining with ·-catenin and glypican-3 was done on an automated immunostaining device using hematoxylin as counterstaining.

EdU was detected according to manufacturer's recommendations using the Klick-it EdU imaging kit (C10338, Invitrogen) on cryosections with DAPI counterstaining.

Statistics

Groups of two were analyzed by t-test, or, when non-parametric, by the Mann-Whitney test. Comparison between more than two groups was done by ANOVA. Statistical analysis was performed using PRISM version 6.0 software (Graph Pad software). Statistical significance was assumed with p value <0.05 (*), $p<0.01$(**) and $p<0.001$(***). Bars in graphs represent mean and ±SEM for the group. Group size (n) represents biological samples and not experimental sample size.

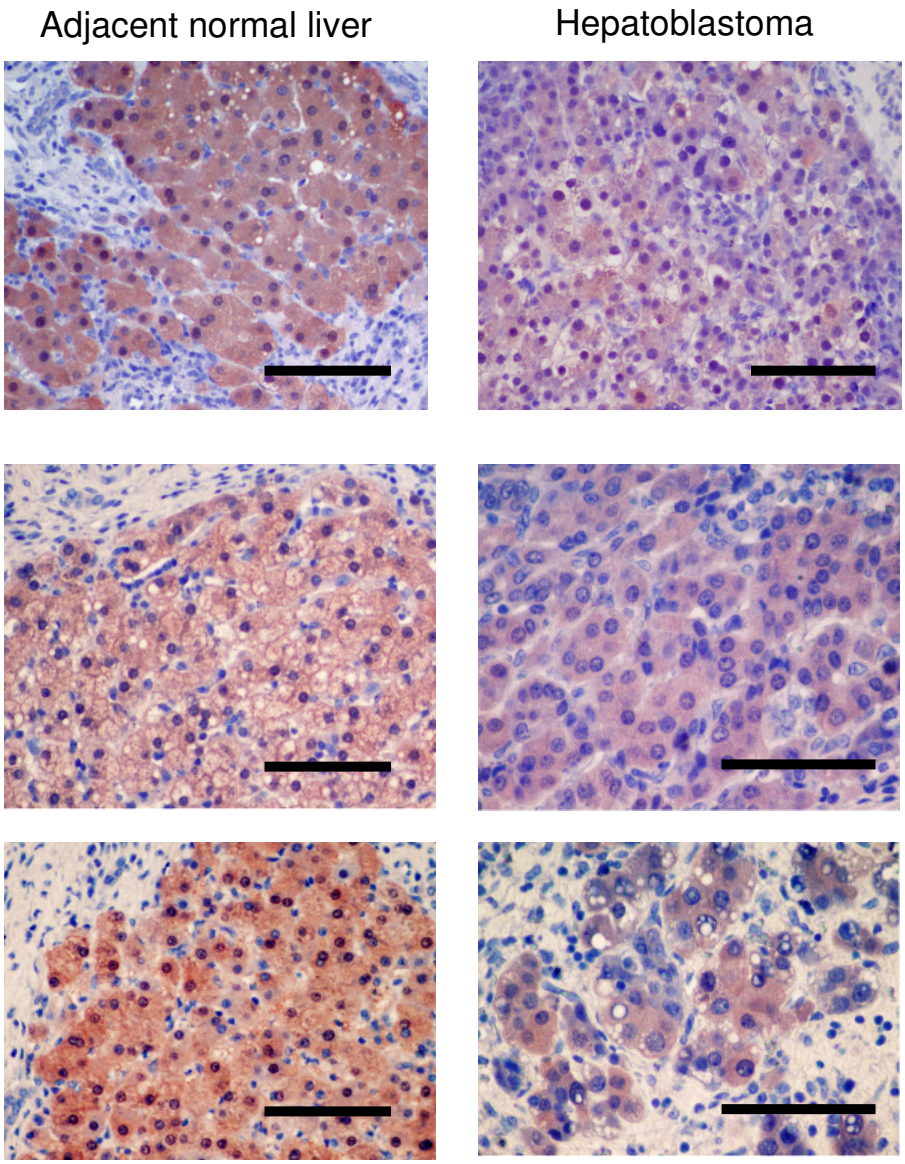

Supplementary Fig. 1. FAH immunostaining in normal liver and tumor tissue of hepatoblastoma patients. Three patients (each row) were evaluated for immunostaining of FAH; normal hepatocytes (left panels) and tumor tissue (right panels). Scale bar is 50 μm.

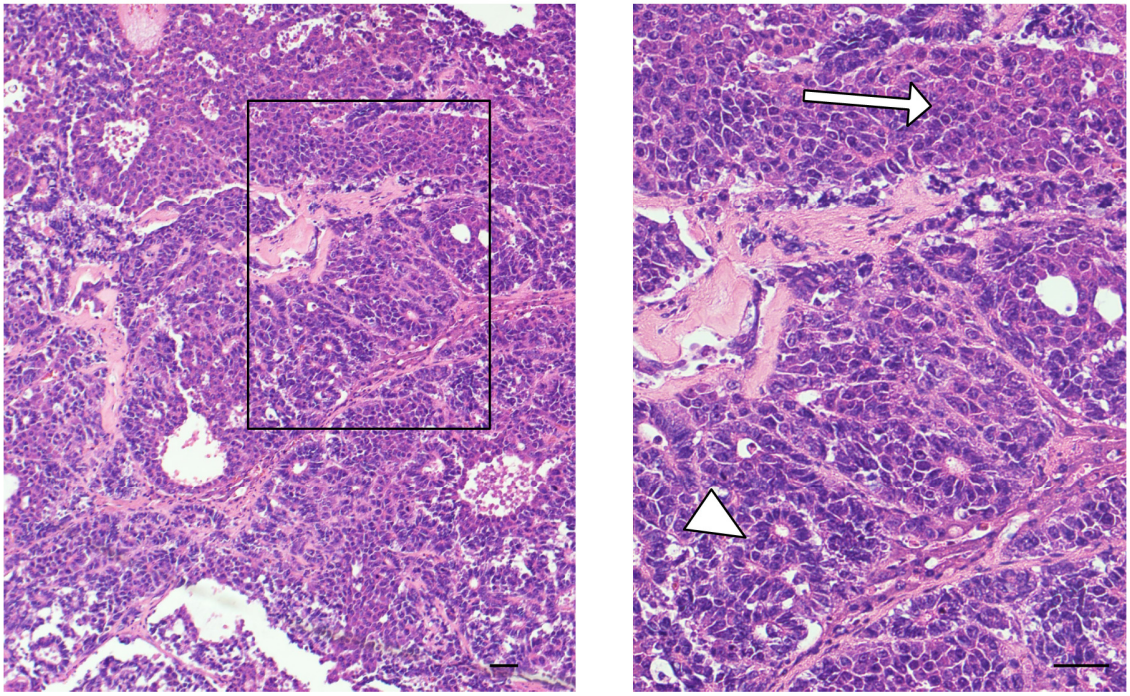

Supplementary Fig. 2. Preservation of embryonal and fetal hepatoblastoma after serial transplantation. PDTX from patient #1 demonstrating embryonal (arrowhead) and fetal (arrow) hepatoblastoma after serial passaging seven times. Right panel is a higher magnification of the boxed inset in the left panel. Scale bar is 50 µm.

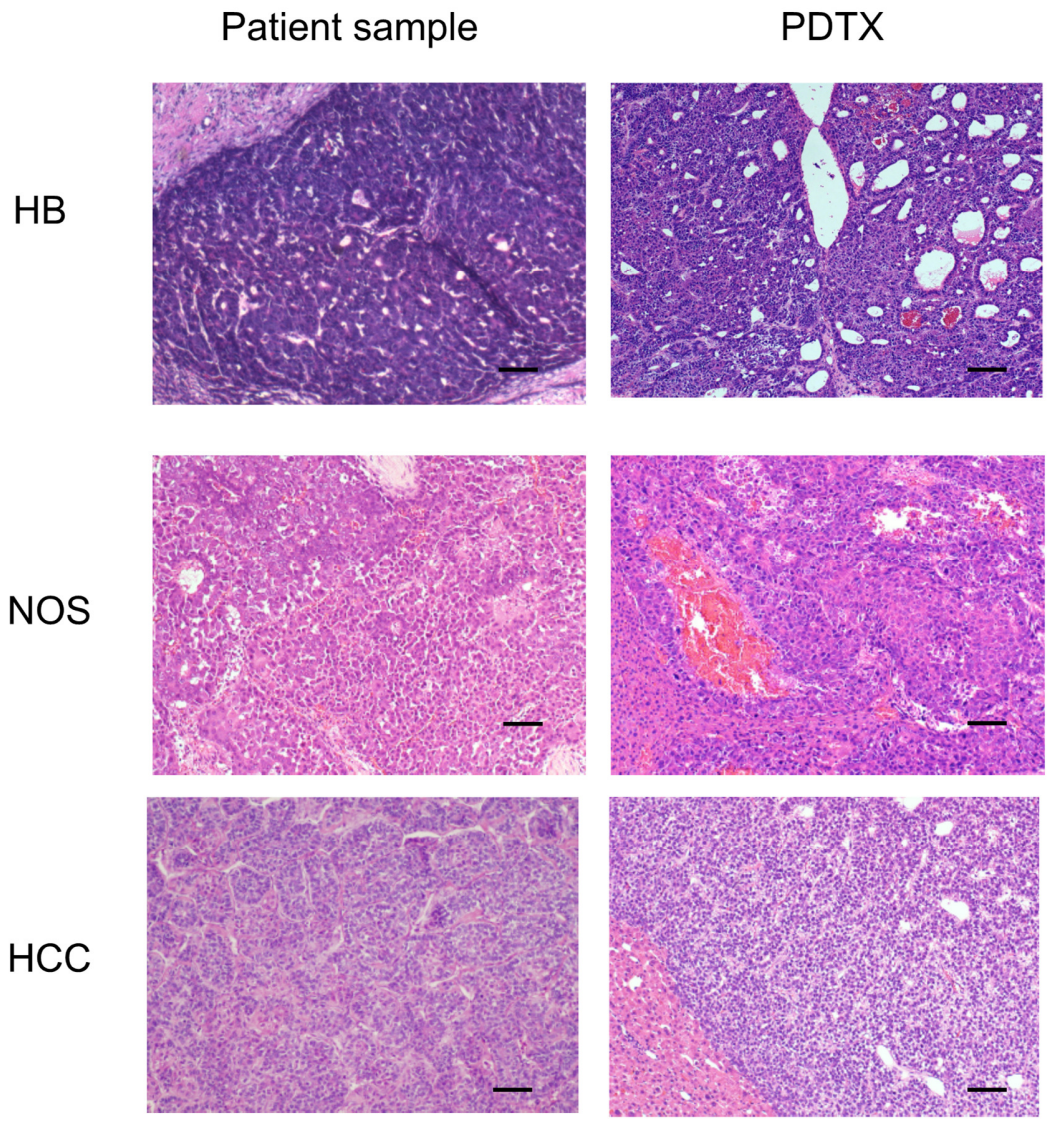

Supplementary Fig. 3. Comparison primary patient sample to PDTX model for multiple histological subtypes of liver cancer. H&E staining revealing similar histological morphology in the original patient tumor compared to the PDTX in three different subtypes: patient #1 is a mixed epithelial hepatoblastoma (HB) patient #2 is a hepatocellular malignant neoplasm (NOS), and patient #12 is a hepatocellular carcinoma (HCC) patient. Scale bar is 50 µm.

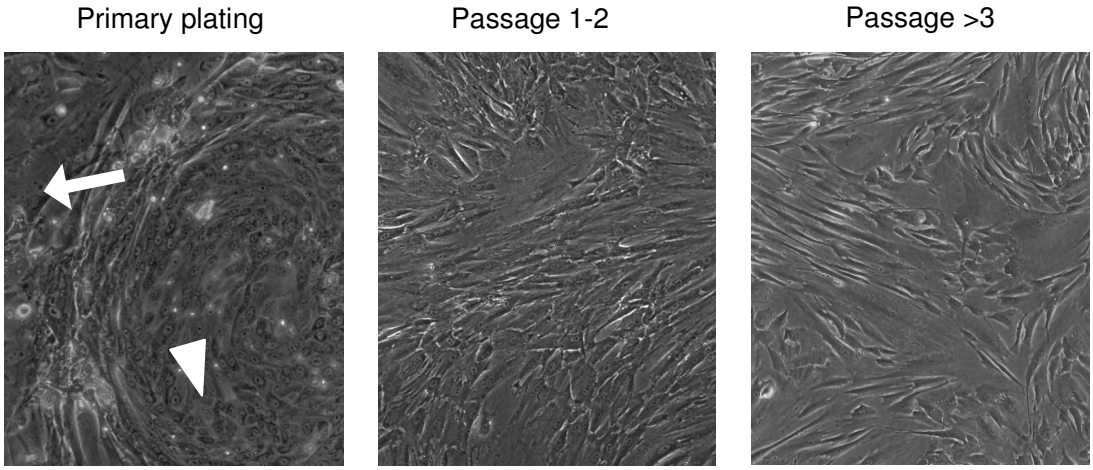

Supplementary Fig. 4. Epithelial cancer cell morphology disappears after passaging when applying standard tissue culture techniques. Phase contrast images of a representative pattern observed when plating primary tumor samples (depict images from patient #3). Arrow point to mesenchymal and arrowhead to epithelial outgrow observed a few days after plating. Morphology of culture changes upon passaging and eventually the whole plate contains only mesenchymal cells. Magnification 200x

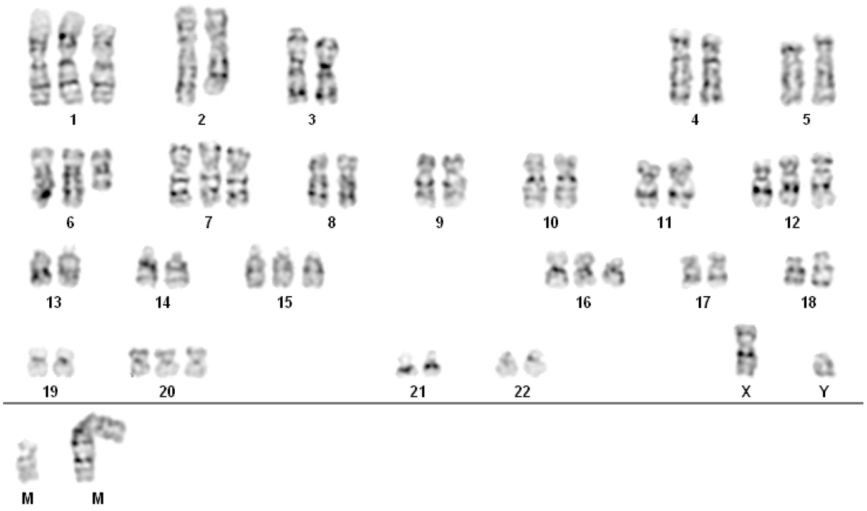

Supplementary Fig. 5. Karyotype cell line (B6-1) of patient #1. Karyotype demonstrates an abnormal chromosome analysis with a hyperdiploid clone (50~51 count) showing additional copies and isochromosome 1q with 1q deletion, and two 6p isochromosomes, as well as deletion of a chromosome 2q region, trisomies of chromosomes 7, 12, 15, 16 and 20 and a variable number of marker chromosomes (M1-8) . The composite karyotype (cp) was generated based on all occurring clonal aberrations in total of fifteen analyzed metaphase cells. Original tumor sample karyotype was not available.

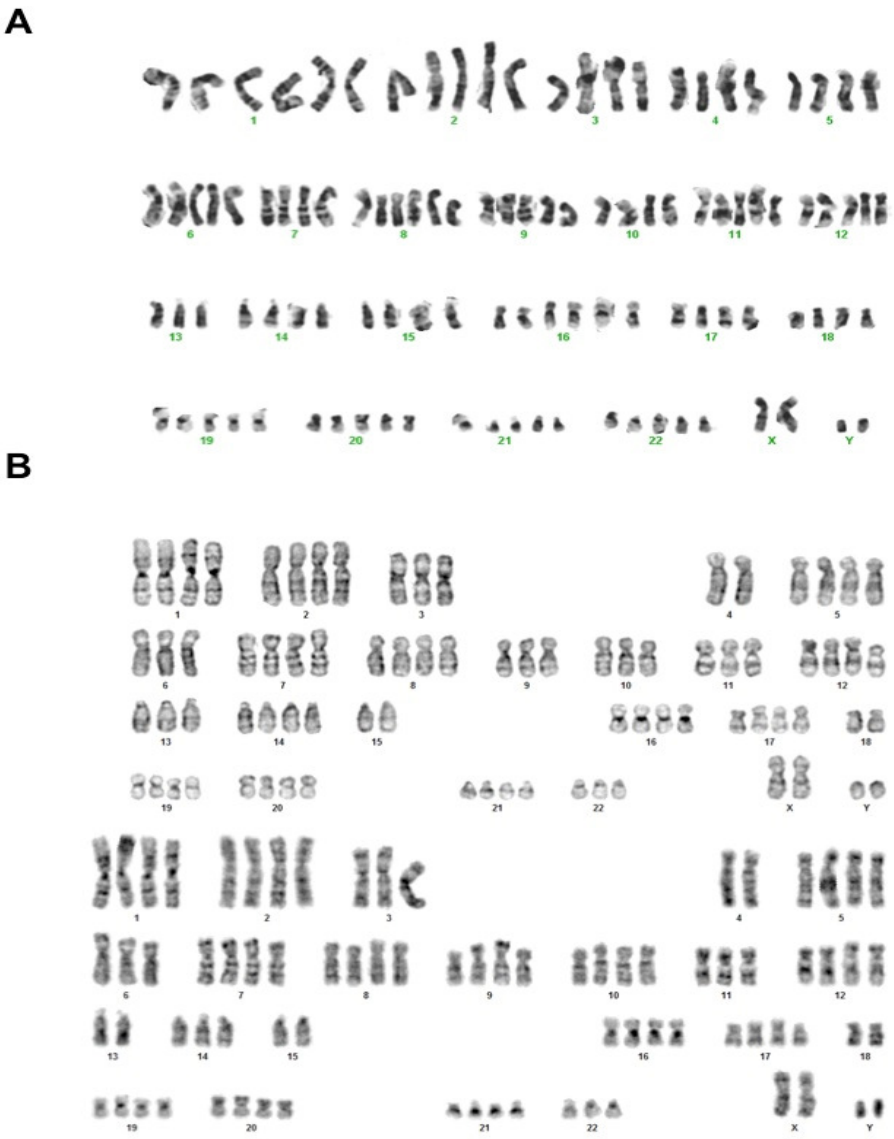

Supplementary Fig. 6. Karyotype cell line (B6-2) and original tumor of patient #2. (A) Original tumor shows abnormal chromosome analysis showing near-pentaploidy clone (105~106 count) in 5 out of 20 cells examined. Gain of chromosomes 2, 8 and 16, loss of chromosomes X, 3, 4, 5, 7, 10, 13, 14, 15, 18 and 21, as well as two copies of an isochromosome of the 1 q-arm (in addition to

four normal copies of 1), were observed. (B) B6-2 (subclone B6-2B) cell line derived from patient #2 showed abnormal male karyotype with clonal structural aberrations including isochromosome for the long arm of chromosome 1 and a translocation between 7p21 and 12p13. In addition, several clonal chromosomal losses were identified in the genomic complement. The composite karyotype (cp) was generated based on all occurring clonal aberrations in total of nine analyzed metaphase cells. Original sample and cell line show important similarities such as trisomies on chromosomes 2, 8 and 9 typical for HB and isochromosme i(1)(q10) encountered in both HB and HCC.

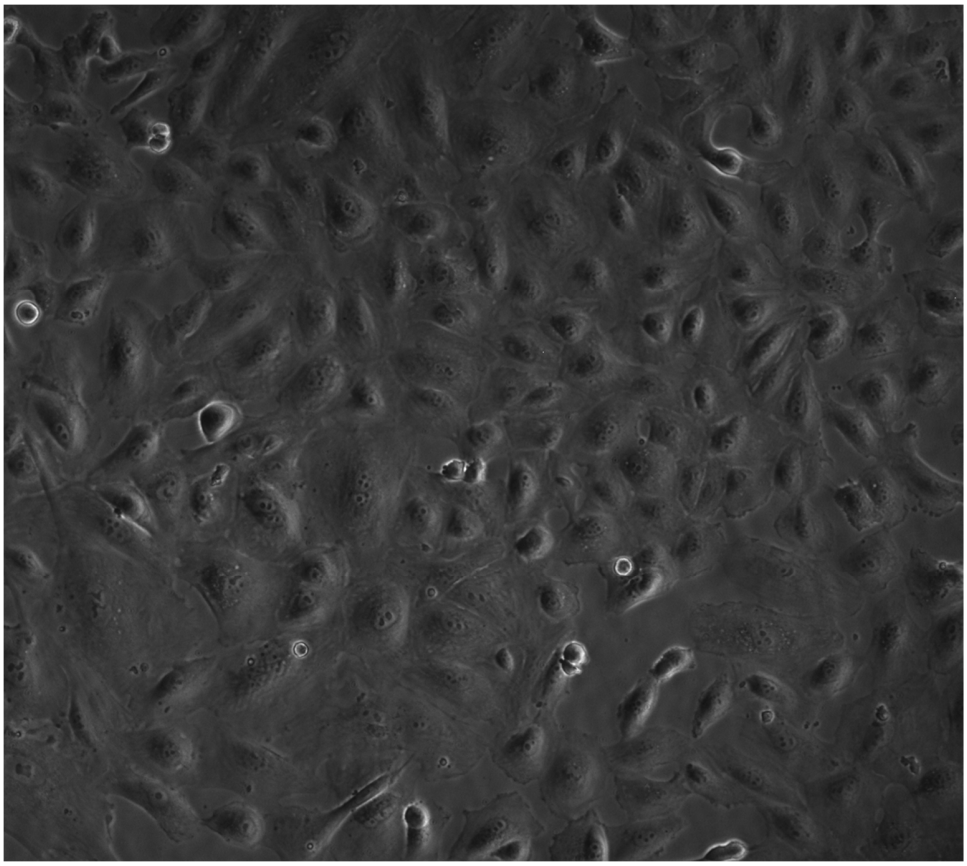

Supplementary Fig. 7. B6-2B cell line growing in standard tissue culture conditions. This subclone could be adapted to standard tissue culture conditions, hence growing in standard media (DMEM, 10% FCS, NEAA) without matrigel coating and passaging in single cell suspension. More than 20 passages have been performed under these conditions. Magnification 400x

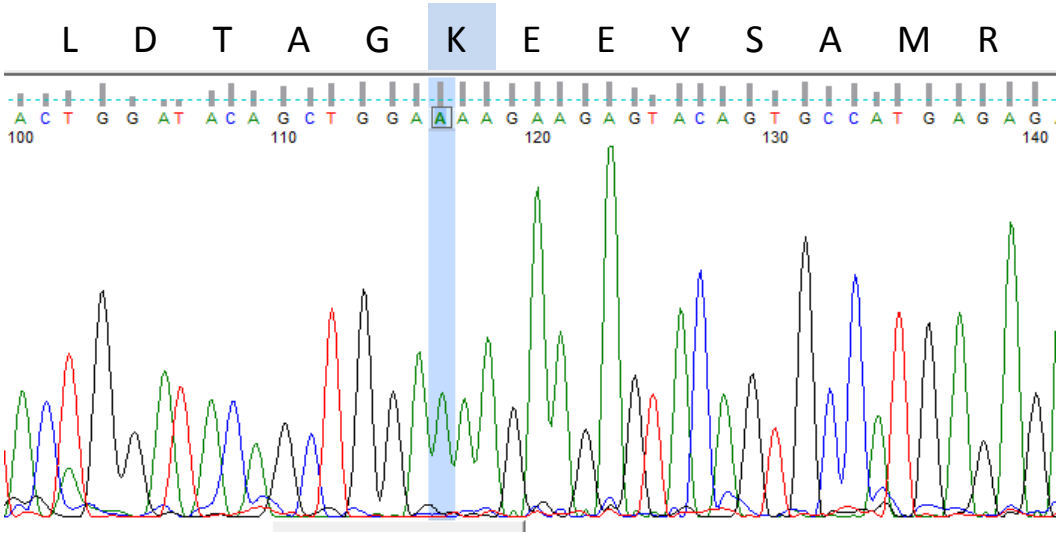

Supplementary Fig. 8. Activating NRAS Q61K mutation in B6-2 cell lines.

Chromatogram showing c181A (genetic) resp. Q61K (protein) mutation in Sanger sequencing reaction.

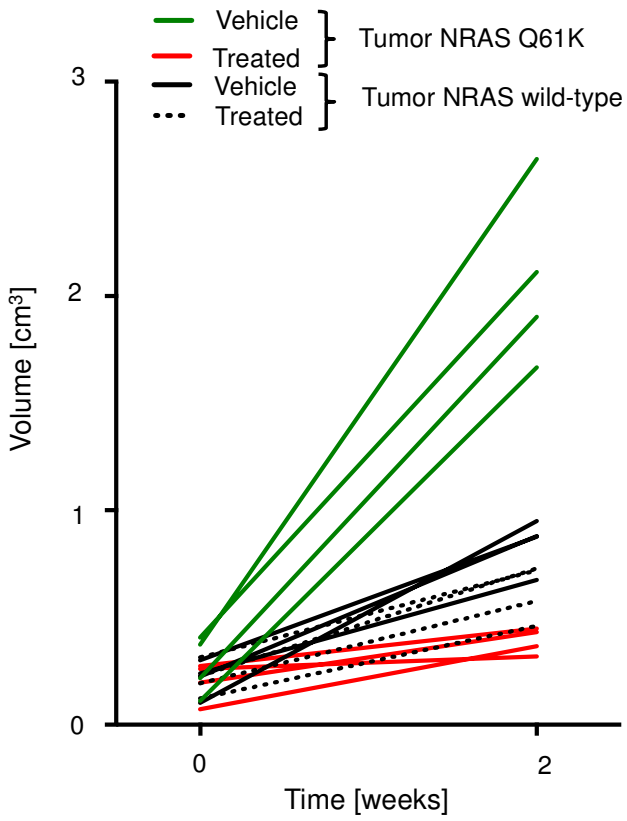

Supplementary Fig. 9. MRI-based volumetry of tumors. NRAS Q61K (colored) and NRAS wild-type (black) tumors before and two weeks after treatment with buparlisib and trametinib or vehicle only. Each line represents an individual animal.

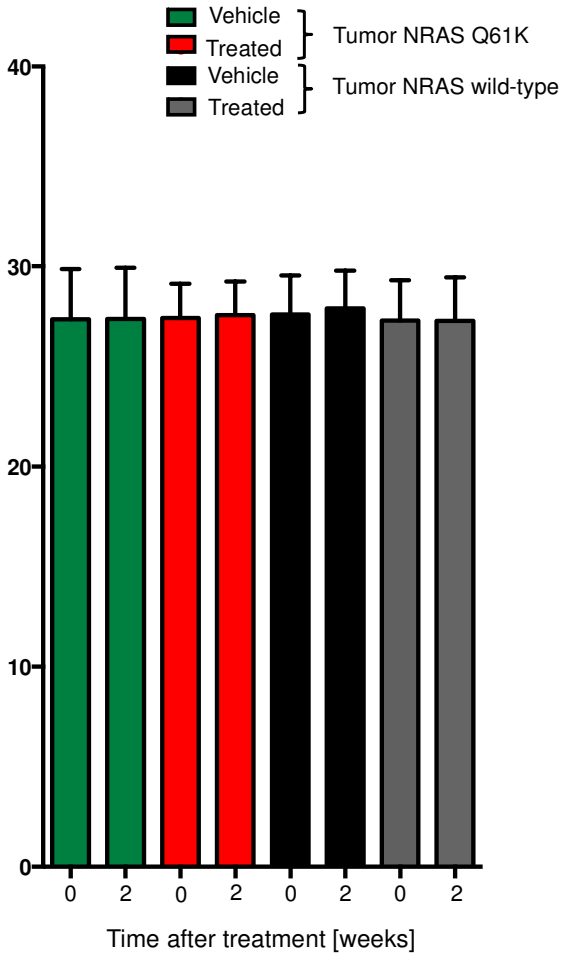

Supplementary Fig. 10. Weights of mice during drug treatment. Wild-type and Q61K NRAS tumors before and two weeks after treatment with buparlisib and trametinib or vehicle only. Bars in graph represent mean ±SEM for the group (n=4).

References:

[1] Shultz LD, Lyons BL, Burzenski LM, Gott B, Chen X, Chaleff S, et al. Human lymphoid and myeloid cell development in NOD/LtSz-scid IL2R gamma null mice engrafted with mobilized human hemopoietic stem cells. J Immunol 2005;174:6477-6489.

[2] Ishikawa F, Yasukawa M, Lyons B, Yoshida S, Miyamoto T, Yoshimoto G, et al. Development of functional human blood and immune systems in NOD/SCID/IL2 receptor {gamma} chain(null) mice. Blood 2005;106:1565-1573.

[3] **Ito M, Hiramatsu H**, Kobayashi K, Suzue K, Kawahata M, Hioki K, et al. NOD/SCID/gamma(c)(null) mouse: an excellent recipient mouse model for engraftment of human cells. Blood 2002;100:3175-3182.

[4] Yahata T, Ando K, Nakamura Y, Ueyama Y, Shimamura K, Tamaoki N, et al. Functional human T lymphocyte development from cord blood CD34+ cells in nonobese diabetic/Shi-scid, IL-2 receptor gamma null mice. J Immunol 2002;169:204-209.

[5] Bissig KD, Le TT, Woods NB, Verma IM. Repopulation of adult and neonatal mice with human hepatocytes: a chimeric animal model. Proc Natl Acad Sci U S A 2007;104:20507-20511.

[6] Azuma H, Paulk N, Ranade A, Dorrell C, Al-Dhalimy M, Ellis E, et al. Robust expansion of human hepatocytes in Fah(-/-)/Rag2(-/-)/Il2rg(-/-) mice. Nat Biotechnol 2007;25:903-910.

[7] Yang Y, Muzny DM, Reid JG, Bainbridge MN, Willis A, Ward PA, et al. Clinical whole-exome sequencing for the diagnosis of mendelian disorders. N Engl J Med 2013;369:1502-1511.

[8] Yang Y, Muzny DM, Xia F, Niu Z, Person R, Ding Y, et al. Molecular findings among patients referred for clinical whole-exome sequencing. JAMA 2014;312:1870-1879.

[9] Bainbridge MN, Wang M, Wu Y, Newsham I, Muzny DM, Jefferies JL, et al. Targeted enrichment beyond the consensus coding DNA sequence exome reveals exons with higher variant densities. Genome Biol 2011;12:R68.

[10] Reid JG, Carroll A, Veeraraghavan N, Dahdouli M, Sundquist A, English A, et al. Launching genomics into the cloud: deployment of Mercury, a next generation sequence analysis pipeline. BMC Bioinformatics 2014;15:30.

[11] Forbes SA, Beare D, Gunasekaran P, Leung K, Bindal N, Boutselakis H, et al. COSMIC: exploring the world's knowledge of somatic mutations in human cancer. Nucleic Acids Res 2015;43:D805-811.

[12] Robinson JT, Thorvaldsdottir H, Winckler W, Guttman M, Lander ES, Getz G, et al. Integrative genomics viewer. Nat Biotechnol 2011;29:24-26.

Author names in bold designate shared co-first authorship